

This is the peer reviewed version of the following article:

Pulsed current effect on hard anodizing process of 7075-T6 aluminium alloy / Bozza, Andrea; Giovanardi, Roberto; Manfredini, Tiziano; Mattioli, Paolo. - In: SURFACE & COATINGS TECHNOLOGY. - ISSN 0257-8972. - ELETTRONICO. - 270:(2015), pp. 139-144. [10.1016/j.surfcoat.2015.03.010]

Terms of use:

The terms and conditions for the reuse of this version of the manuscript are specified in the publishing policy. For all terms of use and more information see the publisher's website.

10/01/2026 11:49

Accepted Manuscript

Pulsed Current Effect On Hard Anodizing Process Of 7075-T6 Alluminium Alloy

Andrea Bozza, Roberto Giovanardi, Tiziano Manfredini, Paolo Mattioli

PII: S0257-8972(15)00199-1
DOI: doi: [10.1016/j.surfcoat.2015.03.010](https://doi.org/10.1016/j.surfcoat.2015.03.010)
Reference: SCT 20154

To appear in: *Surface & Coatings Technology*

Received date: 10 December 2014
Accepted date: 4 March 2015



Please cite this article as: Andrea Bozza, Roberto Giovanardi, Tiziano Manfredini, Paolo Mattioli, Pulsed Current Effect On Hard Anodizing Process Of 7075-T6 Alluminium Alloy, *Surface & Coatings Technology* (2015), doi: [10.1016/j.surfcoat.2015.03.010](https://doi.org/10.1016/j.surfcoat.2015.03.010)

This is a PDF file of an unedited manuscript that has been accepted for publication. As a service to our customers we are providing this early version of the manuscript. The manuscript will undergo copyediting, typesetting, and review of the resulting proof before it is published in its final form. Please note that during the production process errors may be discovered which could affect the content, and all legal disclaimers that apply to the journal pertain.

PULSED CURRENT EFFECT ON HARD ANODIZING PROCESS OF 7075-T6 ALLUMINIUM ALLOY

* Andrea Bozza^a, Roberto Giovanardi^a, Tiziano Manfredini^a, Paolo Mattioli^b

^aUniversity of Modena e Reggio Emilia, Department of Engineering 'Enzo Ferrari', Via Vivarelli 10, 41125
Modena, ITALY

^bMicrontech s.r.l., GPS-Mochem group, Via A. Boito 431, 41019 Soliera (MO), ITALY

ABSTRACT

The aim of this work is to study the influence of pulsed current on hard anodizing process (in sulphuric acid bath) of AA 7075-T6, a commercial heat treated aluminium alloy widely used in several innovative and strategic mechanical sectors (military, automotive, aerospace, etc). Exploiting different pulsed current procedures (slow square pulse mode), combining different duty cycles and current levels it was possible to obtain thick and hard anodic oxides with a good interfacial adhesion. The optical microscopy characterization shows that the use of pulsed current minimizes the growth of defects at the oxide/alloy interface caused by the presence of intermetallic precipitates characteristic of AA 7075-T6. Moreover nano-indentation profiles, evaluated along the coatings cross section, highlight the oxide hardness increase of the samples obtained employing pulsed current cycles (PC) compared to those obtained with standard direct current process (DC) or multistep direct current procedures (MSDC).

Keywords: hard anodizing, pulsed current, aluminium, intermetallics

* author to whom correspondence should be addressed, e-mail: andrea.bozza1989@gmail.com

1. INTRODUCTION

Hard anodizing represents an interesting and useful treatment able to confer, to aluminium alloys, high surface mechanical properties such as good micro-hardness and wear resistance in addition to the essential protective and corrosion resistance properties closely related to the nature of the aluminium oxide [1].

The main difficulties found during the anodizing process are usually related to the compositional heterogeneity of aluminium alloys which is even more accentuated in the heat treated alloys (such as AA 7075-T6) in which the increase in mechanical strength is guaranteed by the formation of several intermetallic precipitates [2].

Defects arising from intermetallics (compounds characterized by a composition rich of alloying elements, such as Cu, Fe, Mn, Mg, Si), affect both decorative and hard anodizing in which, due to higher currents and lower bath temperatures, the risk of failure of the treatment is even more considerable.

The more critical flaws concern with the different current distribution of the electric field between the alloy matrix and the intermetallic phases which usually leads, mostly at the high voltage values reached in the final stages of the treatment, to an uneven growth of the anodic oxide (sometimes referred as conical asperity [1,3]) and causes the entrapment of unoxidized metal particles in the coating (Al-Fe-Mn-Si intermetallic phases) [1,3-8]. Other well-known defects, still related with intermetallic precipitates, are represented by sites that enhance the oxygen evolution process, a parasite reaction which both decreases the faradic efficiency of the treatment and tends to deteriorate the interfacial adhesion of the oxide layer (Al-Cu-Fe intermetallic phases) [9,10,11].

In thermally aged Al-Zn-Mg-Cu alloys of the 7000 series usually both the aforementioned intermetallic phases [6,7,12] are present, and that makes the AA 7075-T6 difficult to be promisingly hard anodized; in particular it's difficult to ensure a good micro-hardness/adhesion relationship.

The optimization of the oxide/alloy interfacial adhesion is necessary in the attempt to decrease the inevitably worsening of anodized components fatigue properties [13,14] and fretting resistance [15] due to the coating brittleness. The coating interface quality is industrially often guaranteed applying lower current density (even only for an initial period) and setting higher bath temperature in order to homogenize the oxide growth thanks to a more gradual potential increase. Unfortunately this strategy often cause the growth of a soft and porous oxide not suitable for critical applications.

Some research have focused on avoiding to anodize directly the alloy by depositing a thin pure PVD-Al layer before anodizing [15]; other studies were done to evaluate the role of Fe-Si impurities characterizing different AA 7075-T6 extrusion products, establishing how compositions with low percentages of silicon and iron can be better anodized [6,7] and testing how a stronger electrolytic solution can partially counteract the effects of these precipitates by dissolving them [6].

In the present work pulsed current (using slow square mode) and multistep direct current anodizing were performed in order to assess their influence on hard anodizing of AA 7075-T6 trying to increase the anodic oxide hardness without affecting their interfacial adhesion, thus limiting the defects expansion in correspondence of the intermetallic phases.

Important studies on pulse anodizing in different electrolytic baths have dealt with easier anodizable alloys (e.g. 1000 and 6000 series) to exploit the recovery effect [16] and the improvement in term of heat dissipation, in order to provide higher current densities and therefore decreasing the process time [17], obtaining oxides comparable or superior to those obtained in DC [18]. Other studies have instead examined the effect of pulsed current on casting alloys, poorly anodizable substrates due to the presence of high concentration of fluidity modifier elements (such as Si and Cu); these works [19], focused on the possibility of delivering different waveforms currents, were able to obtain good anodic oxides but highlighted how it is difficult judging the effects of pulse anodizing process on multiphase

alloys. The entire history of pulsed anodizing and its main advantages were well reviewed by V. Raj *et al.* in 2003 [20].

The aim of this work on pulse anodizing is to take advantage of *time off* intervals at lower current densities in order to homogenize the AA 7075-T6 anodic oxide growth, allowing a better heat dissipation, restoring the electrical double layer and facilitating the removal of the oxygen developed on some precipitates.

Obtaining thick oxides, with a greater compactness and an improved interfacial adhesion, represents an interesting possibility to use the mechanically performing 7075-T6 alloy in even more critical applications wherein the surface tribological properties of the component play a key role.

2. MATERIAL AND METHODS

2.1 Hard anodizing tests

All the anodizing procedures were performed using the laboratory anodizing system shown in Figure 1 consisting of a galvanostat-potentiostat (AMEL Instrument 2055) equipped with a programmable functions generator (AMEL Instrument 568) (element 1), an ammeter (element 2), a voltmeter (element 3) (Keithley 2000) and a thermostated anodizing cell (element 4). The cell consists of a cathode in AA 6060 (element 5), a AA 7075-T6 disc (14 mm of diameter and 3 mm of thickness), inserted in a suitable sample holder (exposed surface 1.0 cm²), as working electrode (element 6).

The cooling and the agitation of the solution, key parameters of the hard anodic oxidation, were carried out through a thermocryostat (Julabo F32) and an air agitation system (element 7 and 8 respectively): the bath temperature was also monitored by a thermometer immersed in the solution.

Preliminary tests were performed in order to optimize the bath composition by preparing electrolytic solutions (element 9) with H_2SO_4 (concentration ranging between 140 – 240 g/L) and a source of Al^{3+} (concentration ranging between 2 – 10 g/L): the addition of aluminium ions simulate the natural aging of an industrial bath caused by the slightly anodic dissolution of aluminium parts during the anodizing process. These experiments allowed to identify an optimal bath composition for the hard anodizing process of AA 7075-T6 by setting 190 g/L as H_2SO_4 concentration and Al^{3+} ranging between 5 – 8 g/L (a change of Al^{3+} concentration within this range doesn't significantly affect the anodizing results).

The use of simple air agitation and the addition of Al^{3+} (simulating the industrial bath aging) ensure that the information obtained on laboratory scale are well transferable to the industrial practice while the programmable functions generator and the controlled exposed area allow to perform pulse anodizing (setting i_{on} , i_{off} , t_{on} and t_{off} values) and to evaluate the faradic efficiency and the volumetric expansion ratio of the coatings, in order to study in more detail the properties of the oxides obtained.

The different procedures tested and their settings are summarized in Table I and Table II; DC (Direct Current), MSDC (Multistep Direct Current) and PC (Pulsed Current, slow square pulse mode) abbreviations are used.

The charge transferred during each procedure was monitored by the ammeter: the samples which reached the voltage limit of the apparatus (72 V) were characterized by the consequent current decreasing and a less total charge transferred compared with the theoretical calculated charge of 136.8 C selected as common point for all the tests performed.

2.2 Characterization techniques

The anodic oxides obtained were characterized by recording and analysing data concerning:

- i) L^* parameter of the CIELAB colour space indicative of the coating darkness usually related to the oxide compactness (the darker the oxide, and so the lower the lightness L^* , the higher

the mechanical properties), acquired with the spectrophotometer X-rite series SP60; each value is an average of seven measures acquired at least two hours after the rinsing of the sample with water in order to ensure the sealing of the oxide in atmospheric conditions;

ii) coating thickness and alloy/oxide interfacial adhesion quality (type and dimension of defects) evaluated by microscopy analysis of the oxides cross sections using a Metallographic Optical Microscope (LEICA DMI5000M); to expose the cross section the samples were embedded in epoxy resin, cut with Struers Labotom-3, and polished with emery papers and a diamond suspension (3 μm);

iii) faradic efficiency calculated as a ratio of the experimental converted mass, m_{ex} (evaluated measuring the depth of the converted alloy from the section micrograph corresponding to the gasket/sample contact zone, as shown in Figure 2 by the line 'Al') and the theoretical mass, m_{th} , of the anodized alloy (i.e. the mass of alloy theoretically converted into oxide, obtained by Faraday Law considering the total charge transferred during the experiment). Formula (1) summarizes the aforementioned calculation:

$$\eta\% = \frac{m_{\text{ex}}}{m_{\text{th}}} = \frac{(Al) \times (surface\ area) \times density}{MQ/zF} \times 100 \quad (1)$$

where M is the material molar mass evaluated considering the 7075 alloy composition (28.27 g/mol, [21]), Q the total charge transferred during the experiment (expressed in Coulombs), z is the number of electrons exchanged during the oxidation reaction (2.92225 for the AA 7075, [21]) and F the Faraday constant (96485 C/mol). The alloy density and the surface exposed area were 2.81 g/cm³ and 1.0 cm² respectively;

iv) volumetric expansion ratio ($V_{\text{ox}}/V_{\text{met}}$), as presented in the following Formula (2) and inspired by some literature works [22,23], based on a simple measure of the alloy converted depth ('Al' line in Figure 2) and the oxide thickness ('Ox' line in Figure 2):

$$Volumetric\ expansion\ ratio = \frac{V_{\text{ox}}}{V_{\text{met}}} = \frac{Ox\ thickness \times surface\ area}{Al\ converted\ depth \times surface\ area} \quad (2)$$

The latter quantity, being compared with the theoretical limit of pure alumina (Pilling-Bedworth ratio of 1.275) is useful to evaluate the oxide compactness and porosity;

v) nano-hardness profiles acquired along the oxides cross section using a CSM Nanoindentation Tester equipped with a Berkovich tip and setting a maximum load of 50 mN, a loading/unloading speed of 40 mN/min and 15 s as dwell time. The reported values, evaluated directly by the software using the Oliver-Pharr method [24], derive from three nano-hardness profiles each consisting of five indentations. An average of all the indentations was also reported.

3. RESULTS AND DISCUSSION

3.1 Direct current and multistep DC anodizing

The former part of this work has dealt with the study of the influence of the anodizing bath composition, in particular evaluating H_2SO_4 (anodizing electrolyte) and Al^{3+} (bath contaminant and *hard Lewis's acid*) role and establishing their optimal concentration range during DC hard anodizing. These results, not presented exhaustively in this work, have allowed to understand how the most important effect of these two acid species is the growth of an extremely defected oxide when their concentrations are close or exceed a threshold value (240 g/L for H_2SO_4 and 10 g/L of Al^{3+}). All subsequent anodizing tests were carried out using solutions containing 5 – 8 g/L of Al^{3+} and 190 g/L of H_2SO_4 , which represent the optimal conditions in terms of oxide defectiveness achieved. Natural continuation of the preliminary work was an intense study of the influence of the bath temperature, an even more critical process parameter for the hard anodizing treatment, especially for the peculiar 7075-T6 alloy.

These tests, performed applying direct current (24 mA/cm² for 95 minutes, as summarized in Table I), have allowed to highlight how the brittleness and the poor mechanical properties of

the anodic oxide of the AA 7075-T6 can be ascribed to the alloy/oxide interface defects which grow when not appropriated bath conditions are set, and that are emphasized when high voltage is reached (72 V for the laboratory system employed).

At the higher potential values, sometimes reached during the final anodizing stages (for example if an extremely thick oxide is desired), all the problems related to the different response of the electric field on the intermetallics become more relevant with consequent formation of large interfacial flaws often associated to a critical stress state and the development of gaseous O₂. Setting lower temperatures does not permit an optimal oxygen diffusion toward the oxide facilitating a deep longitudinal cracking on the conical asperity defects (as shown in Figure 3a), while at higher temperatures poor and too porous coatings are obtained (as reported in Table III, at $T > 0^{\circ}\text{C}$), because at the higher temperatures the dissolution effect of the acid bath becomes stronger.

With this analysis was therefore possible to identify -2°C as the most promising anodizing temperature for the AA 7075-T6 even if, by reducing the acid dissolution and accelerating the film growth (respect to 0°C or 2°C), this temperature (DC condition) induces a non linear alloy/oxide interface (Figure 3b).

The first attempts to increase the mechanical performance of the AA 7075-T6 anodic films (i.e. a homogenous growth and a good interfacial adhesion of the oxide) were performed by optimising some multistep direct current procedures (MSDC), realized combining two different levels of current density.

The selection of a first galvanostatic step at low current density (compared to the single level of 24 mA/cm^2 used in the DC procedures previously reported) was performed with the intention to avoid the creation of strong electric field concentrated on the intermetallics during the first instants of oxide growth.

The four procedures adopted are summarized in Table I, while in Table III the characterization results are reported. The introduction of MSDC anodizing procedure allows

to obtain high quality and well adherent coatings: the most performing treatment was obtained combining a first step at 18 mA/cm^2 , maximum 20 minutes long (ramps MSDC_3 and MSDC_4), followed by a second step at 24 mA/cm^2 . The effectiveness of the MSDC procedure can be ascribed to the formation of a first non-defected layer during the first '*low current*' step; during the subsequent '*high current*' step the oxide growth proceeds on both the interfacial fronts of the thin non-defected layer previously formed, avoiding an excessive concentration of the electric field on the intermetallic compounds when the higher currents start flowing.

The extension of the '*low current*' step over 20 minutes brings to the formation of an initial layer of high thickness, compromising the mean hardness of the final oxide obtained, as show in Table III for MSDC_2 experiment (the reason is that the initial layer, grown a low current, is not very hard). This effect is emphasized when a very low current level for the initial step is selected (i.e. 15 mA/cm^2), as show in Table III for MSDC_1 experiment.

The absence of interfaces along the oxide cross sections, that could have been caused by the current increase (current jump or current ramp), indicates a perfect uniformity of the oxides obtained by the optimized MSDC procedure (as shown in Figure 3c) and thus a low risk of coating delamination during use. Anyway the MSDC technique doesn't allow to obtain significant improvements in term of hardness (compared with DC procedures) and when the higher hardness values are reached (310 HV obtained with MSDC_3 experiment) it's not possible to eliminate all the oxide defects (Figure 3c).

3.2 Pulsed current anodizing

The different pulsed current procedures performed changing i_{on} , i_{off} and duty cycles[†] are described in Table II. The application of a slightly anodic current during the *time-off* phase

[†] The duty cycle is the ratio between t_{on} interval and the period (sum of t_{on} and t_{off}). This value, expressed in percentage (DC%), represents the working activity of a defined pulsed current cycle tested.

($i_{\text{off}} = 6 \text{ mA/cm}^2$), selection based on literature data [17-20], ensures some breaks during the growth phase without allowing the development of undesired parasitic reactions (activated, for example, by cathodic polarization). The current values (i_{on}) applied during the working phase (*time-on*) have been chosen considering the previous DC and MSDC tests: 24 mA/cm^2 represents the current level employed in the preliminary analysis while 36 mA/cm^2 intends to be an extreme attempt to optimize the oxide mechanical properties, assuming that higher currents, applied in slow square pulse mode, would provide a discrete heat dissipation and a temporally limited concentration of the electric field on intermetallics.

The characterizations of the oxides obtained with pulse anodizing, summarized in Table IV, were compared with the best results achieved in DC (by simple or multistep procedures).

The more significant improvement obtained with the pulse anodizing technique concern the nano-hardness values measured along the oxide cross sections: their average values are abundantly above the hardness obtained with DC and MSDC cycles as their profiles, shown in Figure 4, testify.

The nano-hardness profile of the sample anodized in DC setting -2°C as bath temperature (DC_2) displays an interesting increasing trend towards the oxide/electrolyte interface which demonstrate a poor compactness of the oxide near the metal/oxide interface (due to the presence of microcracks, see Figure 3b) and an extremely hard oxide near the oxide/electrolyte interface, thanks to a less aggressive acid action at -2°C . The PC profiles, at least in the first 50 microns, are instead much more linear confirming the surprising homogeneity of these oxide and proving the efficiency of the procedures tested in terms of performance advantages.

Similarly improvements in volumetric expansion ratio and L^* parameter data were found: pulsed current anodized oxides in fact turn out to be more compact ($V_{\text{ox}}/V_{\text{met}} \sim 1.7$) and very dark ($L^* \sim 34$) when compared with DC and MSDC coatings. In addition pulsed current

cycles, although are characterized by several slow growth intervals (t_{off}), express good faradic efficiency, typical for this alloy when correctly anodized.

Setting too high DC% (as 91%) or choosing 36 mA/cm^2 as i_{on} , however, do not allow the decrease of the defectiveness at the metal/oxide interface. While in the case of high DC% values these issues (defects) are symptomatic of an electrical cycle too similar to a simple direct current procedure (break intervals too short compared to working periods), in the case of excessive current values applied during the *time-on* (i_{on}) the previously discussed problems related to the intermetallics and the different electric field distribution on them recur. Some information about the PC coatings performances can be predicted already during the anodizing process, through the continuous monitoring of the *potential vs time* trend. Figure 5 shows V vs t curves obtained during anodizing with different electric techniques[‡]: assuring break intervals during *time-off* allows a more gradual oxides growth testified by the absence of abrupt slope variations typical of DC V vs t curves (at the same current level and bath conditions); moreover, with PC_1 and PC_2 procedures it is possible to obtain $80 \mu\text{m}$ thick oxide without reaching extreme voltages (in particular 72 V is the voltage limits for the apparatus employed), thus decreasing the risk of flawed zones.

Optical microscopy images (Figure 6) confirm that when extreme voltage values are reached during anodizing (see PC_5 procedure in Figure 5) the interfacial adhesion of the oxide was compromised by the worsening of the conical asperity defects (Figure 6b), while a lower voltage guarantees a more linear interface (see PC_2 procedure, Figure 5 and Figure 6a); anyway all the PC procedures applied never lead to the longitudinal cracking phenomenon (union of the defects) seen in the case of anodizing at very low temperatures (DC_1 at -5°C , Figure 3a).

Considering that all the PC anodizing treatments tested allow to obtain anodic oxides with a comparable thickness, often exceeding $80 \mu\text{m}$, the idea to perform a specific PC test

[‡] The voltage reported in Figure 5 for PC anodizing is the voltage measured during the time-on intervals (so during the application of i_{on} current)

interrupting it to 40 V in order to decrease the adhesion defects and to lower the process time spontaneously arose (in particular considering that the required thickness for hard anodizing in the industrial practice is often limited to 50 μm).

Stopping the treatment in advance, before to reach extreme voltage values, offers the possibility to obtain linear metal/oxide interfaces for all the PC cycles previously tested: it was therefore chosen to try this strategy for the 36 mA/cm^2 cycle (DC 50%, with both t_{on} and t_{off} of 10 s), which represents a combination between high current density during *time-on* (high risk of flaws) and frequent pauses at low currents (useful for the recovery, the heat dissipation and the homogenization of the temperature on the component).

The sample obtained interrupting the treatment after 76 minutes (before reaching a potential of 40 V) meets all the requirements expected: in just over an hour it was possible to get an hard and compact oxide (PC_6, Table IV) with a defects-free interfacial morphology, shown in Figure 6c, and properties comparable to those of the samples obtained working at lower current values.

4. CONCLUSIONS

The most important results obtained by studying the hard anodizing process of 7075-T6 alloy can be summarized as follow:

- i) the brittleness and the poor interfacial adhesion of the AA 7075-T6 anodic films are related to the presence of some intermetallic phases, which are substrates unfit for this treatment: with direct current procedures (simple DC or MSDC) only a properly selection of the bath conditions and electrical parameters allow the growth of interesting oxides;
- ii) pulsed current cycles (PC), considering slow square pulse mode, allow to obtain hard anodic oxide coating without affecting the interfacial adhesion and then minimizing, thanks to the recovery periods, the flaws growth on the intermetallic phases;

iii) high potential values, reached during the final stage of PC treatments, causes an increase of the defectiveness due to an inhomogeneous concentration of the electric field on the different alloy constituents. Defectless thick coating ($\sim 80 \mu\text{m}$) were obtained applying a current density of 24 mA/cm^2 during the *time-on*, with a duty cycle ranging between 50 and 75 % (120 – 150 minutes treatment); slightly thinner oxides ($50 \mu\text{m}$) can be obtained in 1 hour, interrupting the PC treatment when the voltage approach the value of 40 V.

5. REFERENCES

- [1] P.G Sheasby, R. Pinner, The surface treatment and finishing of aluminum and its alloys, Vol 1 and 2, 6th Edition, ASM International, USA/ Finishing Publications Ltd, UK, 2001.
- [2] M.E. Fine, Precipitation hardening of aluminum alloys, *Metall. Trans. A* 6 (1975) 625-630.
- [3] W.E. Cooke, Factors affecting loss of brightness and image of clarity during anodizing of bright-trim aluminum alloys in sulfuric acid electrolyte, *Plating*, 49 (1962) 1157-1165.
- [4] P.J.E. Forsyth, A three-dimensional study of the microstructure of an aluminium alloy as revealed within its thick anodically formed oxide, *Mater. Lett.* 13 (1992) 184-193.
- [5] P.J.E. Forsyth, Some further observations on the various features of aluminium alloy microstructures that are transferred, bodily, into the oxide coating formed by anodising, *Mater. Lett.* 16 (1993) 113-122.
- [6] A.K. Mukhopadhyay, A.K. Sharma, Influence of Fe-bearing particles and nature of electrolyte on the hard anodizing behaviour of AA 7075 extrusion products, *Surf. Coat. Tech.* 92 (1997) 212-220.
- [7] A.K. Mukhopadhyay, On the nature of the Fe-bearing particles influencing hard anodizing behavior of AA 7075 extrusion products, *Metall. Trans. A* 29A (1998) 979-987.
- [8] L.E. Fratila Apachitei, H. Terryn, P. Skeldon, G.E. Thompson, J. Duszczyk, L. Katgerman, Influence of substrate microstructure on the growth of anodic oxide layers, *Electrochim. Acta* 49 (2004) 1127-1140.
- [9] L. Iglesias-Rubianes, S.J. Garcia-Vergara, P. Skeldon, G.E. Thompson, J. Ferguson, M. Beneke, Cyclic oxidation process during anodizing of Al-Cu alloys, *Electrochim. Acta* 52 (2007) 7148-7157.
- [10] X. Zhou, G.E. Thompson, H. Habazaki, K. Shimizu, P. Skeldon, G.C. Wood, Copper enrichment in Al-Cu alloys due to electropolishing and anodic oxidation, *Thin Solid Films* 293 (1997) 327-332.
- [11] M. Saenz de Miera, M. Curioni, P. Skeldon, G.E. Thompson, The behaviour of second phase particles during anodizing of aluminium alloys, *Corros. Sci.* 52 (2010) 2489-2497.
- [12] N. Birbilis, R.G. Buchheit, Electrochemical characteristics of intermetallic phases in aluminum alloys, *J. Electrochem Soc.* 152 (2005) B140-B151.
- [13] E. Cirik, K. Genel, Effect of anodic oxidation on fatigue performance of 7075-T6 alloy, *Surf. Coat. Tech.* 202 (2008) 5190-5201.
- [14] B. Lonyuk, I. Apachitei, J. Duszczyk, The effect of oxide coatings on fatigue properties of 7475-T6 aluminium alloy, *Surf. Coat. Tech.* 201 (2007) 8688-8694.
- [15] A.A.D. Sarhan, E. Zalnezhad, M. Hamdi, The influence of higher surface hardness on fretting fatigue life of hard anodized aerospace AL7075-T6 alloy, *Mater. Sci. Eng. A* 560 (2013) 377-387.

- [16] K. Yokoyama, H. Konno, H. Takahashi, M. Nagayama, Advantages of pulse anodizing, *Plat. Surf. Finish.* 69 (1982) 62-65.
- [17] A.D. Juhl, Why it makes sense to upgrade to pulse anodizing, *Met. Finish.* 107 (2009) 24-27.
- [18] D. Kanagaraj, V. Raj, S. Vincent, B. Prasanna Kumar, A. Senthil Kumar, S. Venkata Krishna Iyer, Pulse anodizing of AA1100 aluminium alloy in oxalic acid electrolyte, *B. Electrochem.* 17 (2001) 285-288.
- [19] L.E. Fratila-Apachitei, J. Duszczyk, L. Katgerman, AlSi(Cu) anodic oxide layers formed in H₂SO₄ at low temperature using different current waveforms, *Surf. Coat. Tech.* 165 (2003) 232-240.
- [20] V. Raj, M.P. Rajaram, G. Balasubramanian, S. Vincent, D. Kanagaraj, Pulse anodizing – An overview, *T. I. Met. Finish.* 81 (2003) 114-121.
- [21] L. Hao, T. Westre, B.R. Cheng, A comparative study of current and conversion efficiency of the METALAST anodizing processes with and without the METALAST additive, Technical Reports, Metalast International Inc. (2001) 1-22.
- [22] G.E.J. Poinern, N. Ali, D. Fawcett, Progress in nano-engineered anodic aluminum oxide membrane development, *Materials* 4 (2011) 487-526.
- [23] L. Arurault, Pilling-Bedworth ratio of thick anodic aluminium porous films prepared at high voltages in H₂SO₄ based electrolyte, *T. I. Met. Finish.* 86 (2008) 51-54.
- [24] W.C. Oliver, G.M. Pharr, An improved technique for determining hardness and elastic modulus using load and displacement sensing indentation experiments, *J. Mater. Res.* 7 (1992) 1564-1583.

Tables

Table I: Direct Current (DC) and Multistep Direct Current (MSDC) procedures. All the tests were performed in a sulphuric acid bath containing 190 g/L of acid.

Sample	Electrical Parameters			Bath Conditions	
	Initial step	Final step	Duration [min]	Temperature [°C]	Al ³⁺ concentration [g/L]
DC_1	/	24 mA/cm ² for 95 min	95	-5	8
DC_2	/	24 mA/cm ² for 95 min	95	-2	8
DC_3	/	24 mA/cm ² for 95 min	95	0	8
DC_4	/	24 mA/cm ² for 95 min	95	2	8
MSDC_1	15 mA/cm ² for 40 min	24 mA/cm ² for 70 min	110	-2	5
MSDC_2	18 mA/cm ² for 35 min	24 mA/cm ² for 69 min	104	-2	5
MSDC_3	18 mA/cm ² for 10 min	24 mA/cm ² for 87 min	97	-2	5
MSDC_4	18 mA/cm ² for 20 min	24 mA/cm ² for 80 min	100	-2	5

Table II: Pulsed Current (PC) procedures. All PC tests were performed setting 6 mA/cm² as off-current (i_{off}) and 10 s as time-off interval (t_{off}). The bath composition was 190 g/L of sulphuric acid and 5 g/L of Al³⁺; the anodizing temperature was set at -2°C. PC_6 was interrupted just before 40 V.

Sample	Electrical Parameters				Duration [min]
	i_{on} [mA/cm ²]	t_{on} [s]	Duty cycle [DC%]	n° pulses	
PC_1	24	10	50	455	152
PC_2	24	30	75	175	117
PC_3	24	100	91	55	102
PC_4	36	10	50	325	108
PC_5	36	30	75	120	80
PC_6	36	10	50	228	76

Table III: Characterization of the anodic oxides obtained using Direct Current (DC) and Multistep Direct Current (MSDC) procedures.

Sample	Lightness (L*)	Thickness (μm)	$V_{\text{ox}}/V_{\text{met}}$	η (%)	Hardness (HV)	Alloy/oxide interface
DC_1	40.1 ± 0.2	81 ± 2	1.85 ± 0.03	99	260 ± 40	Highly flawed
DC_2	38.2 ± 0.2	82 ± 3	1.72 ± 0.05	99	290 ± 50	Flawed
DC_3	39.4 ± 0.2	82 ± 1	1.76 ± 0.03	94	220 ± 30	Some defects
DC_4	41.8 ± 0.3	80 ± 1	1.85 ± 0.05	89	200 ± 20	Linear
MSDC_1	37.9 ± 0.4	83 ± 1	1.9 ± 0.1	90	230 ± 40	Linear
MSDC_2	36.9 ± 0.5	83 ± 1	1.81 ± 0.03	94	260 ± 40	Linear
MSDC_3	34.8 ± 0.1	81 ± 2	1.79 ± 0.03	93	310 ± 30	Some defects
MSDC_4	38.8 ± 0.2	84 ± 1	1.85 ± 0.02	91	290 ± 40	Linear

Table IV: Characterization of the anodic oxides obtained using Pulsed Current (PC) procedures.

Sample	Lightness (L*)	Thickness (μm)	$V_{\text{ox}}/V_{\text{met}}$	η (%)	Hardness (HV)	Alloy/oxide interface
PC_1	33.3 ± 0.1	79 ± 2	1.7 ± 0.1	90	410 ± 20	Linear
PC_2	33.3 ± 0.1	80 ± 1	1.74 ± 0.02	92	400 ± 20	Linear
PC_3	34.8 ± 0.1	83 ± 3	1.66 ± 0.06	98	380 ± 20	Flawed
PC_4	39.8 ± 0.3	82 ± 2	1.84 ± 0.08	96	420 ± 50	Some defects
PC_5	39.6 ± 0.2	88 ± 2	1.73 ± 0.07	~100	360 ± 10	Flawed
PC_6	34.5 ± 0.2	58 ± 2	1.78 ± 0.03	85	390 ± 30	Linear

Figure Captions

Figure 1: Laboratory anodizing system: 1) galvanostat, 2) ammeter, 3) voltmeter, 4) electrochemical cell, 5) cathode, 6) working electrode, 7) coolant flow, 8) air-agitation system, 9) electrolytic solution.

Figure 2: Micrograph acquired by optical microscope on the cross section of an oxide coating: the gasket/sample contact zone is useful to understand the depth reached by the oxide below the initial level of the alloy: Al represents the depth of the converted alloy, while Ox is the coating thickness.

Figure 3: Micrographs acquired by optical microscope showing the cross section microstructure of oxides obtained using DC_1 (a), DC_2 (b) and MSDC_3 (c) procedures (see Table I). The sample obtained using MSDC_3 procedure was etched with Dix-Keller reagent in order to highlight the correspondence between intermetallics and oxide defects.

Figure 4: Nano-hardness profiles measured along the oxides section.

Figure 5: V vs t curves recorded during the anodizing treatments with different electric techniques: direct current (DC), multistep direct current (MSDC) and pulsed current (PC). In the case of PC anodizing the voltage reported was acquired during the time-on intervals (so during the application of i_{on} current).

Figure 6: Micrographs acquired by optical microscope showing the cross section microstructure of oxides obtained using PC_2 (a), PC_5 (b) and PC_6 (c) procedures (see Table II).

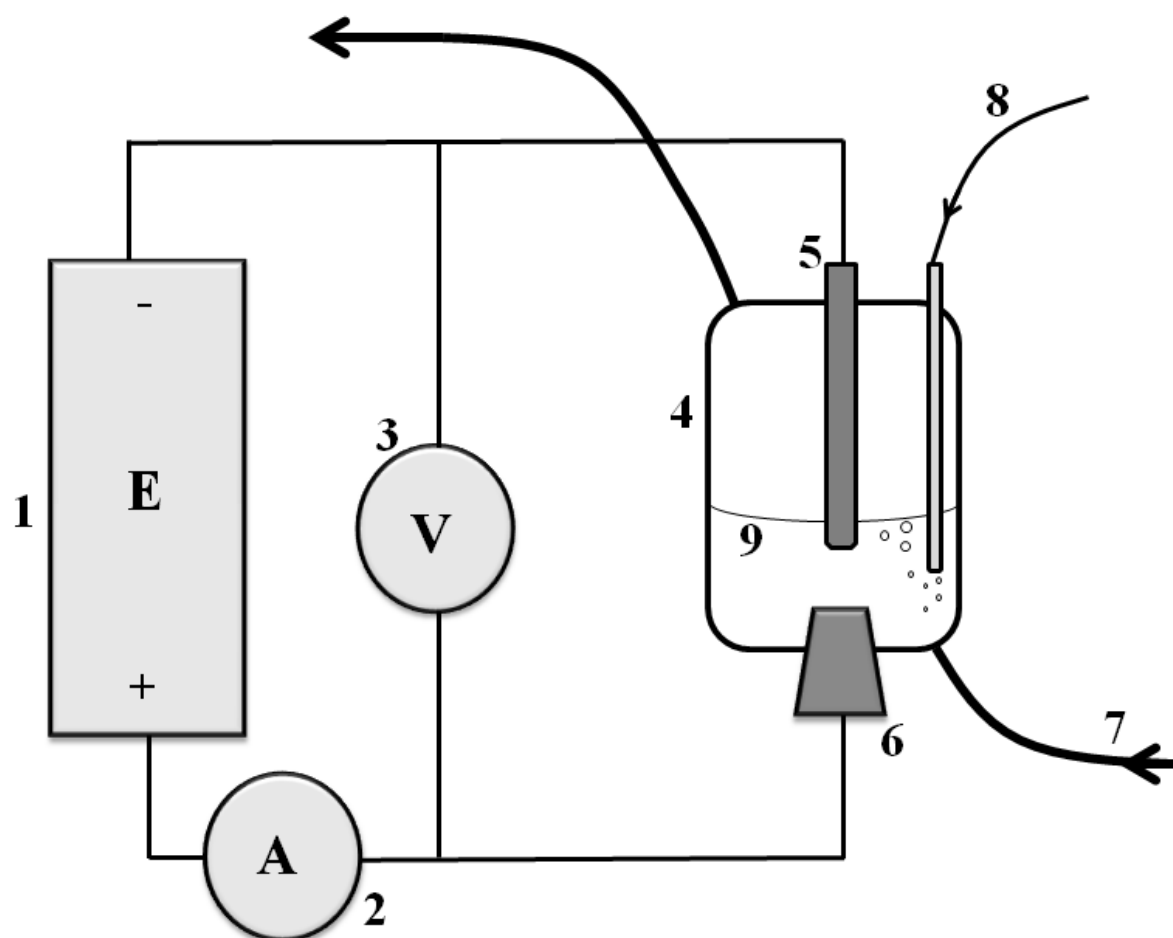


Figure 1

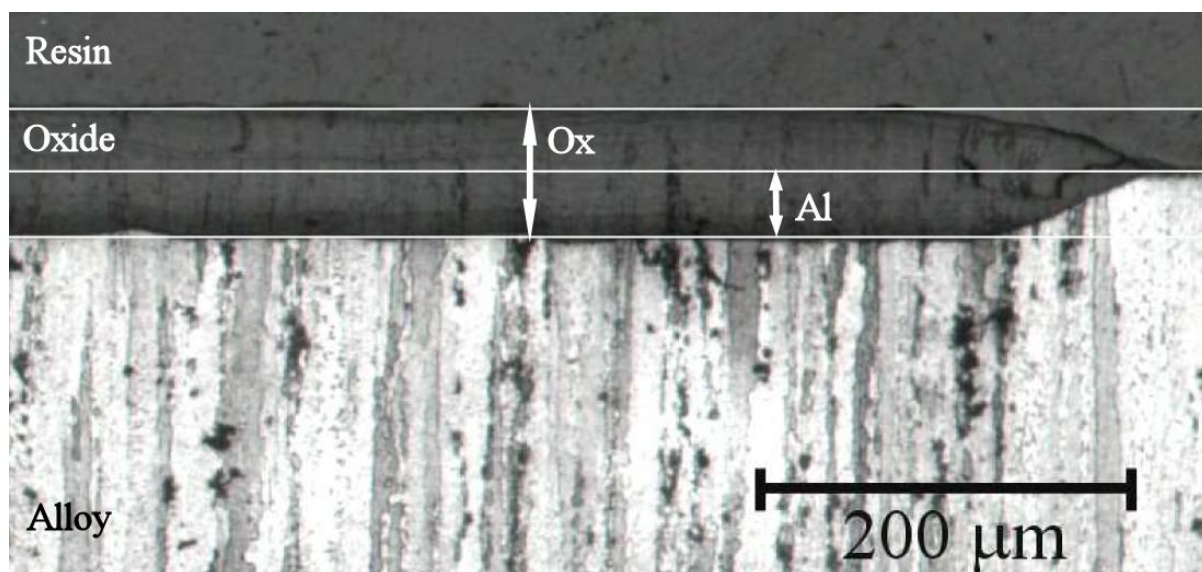


Figure 2

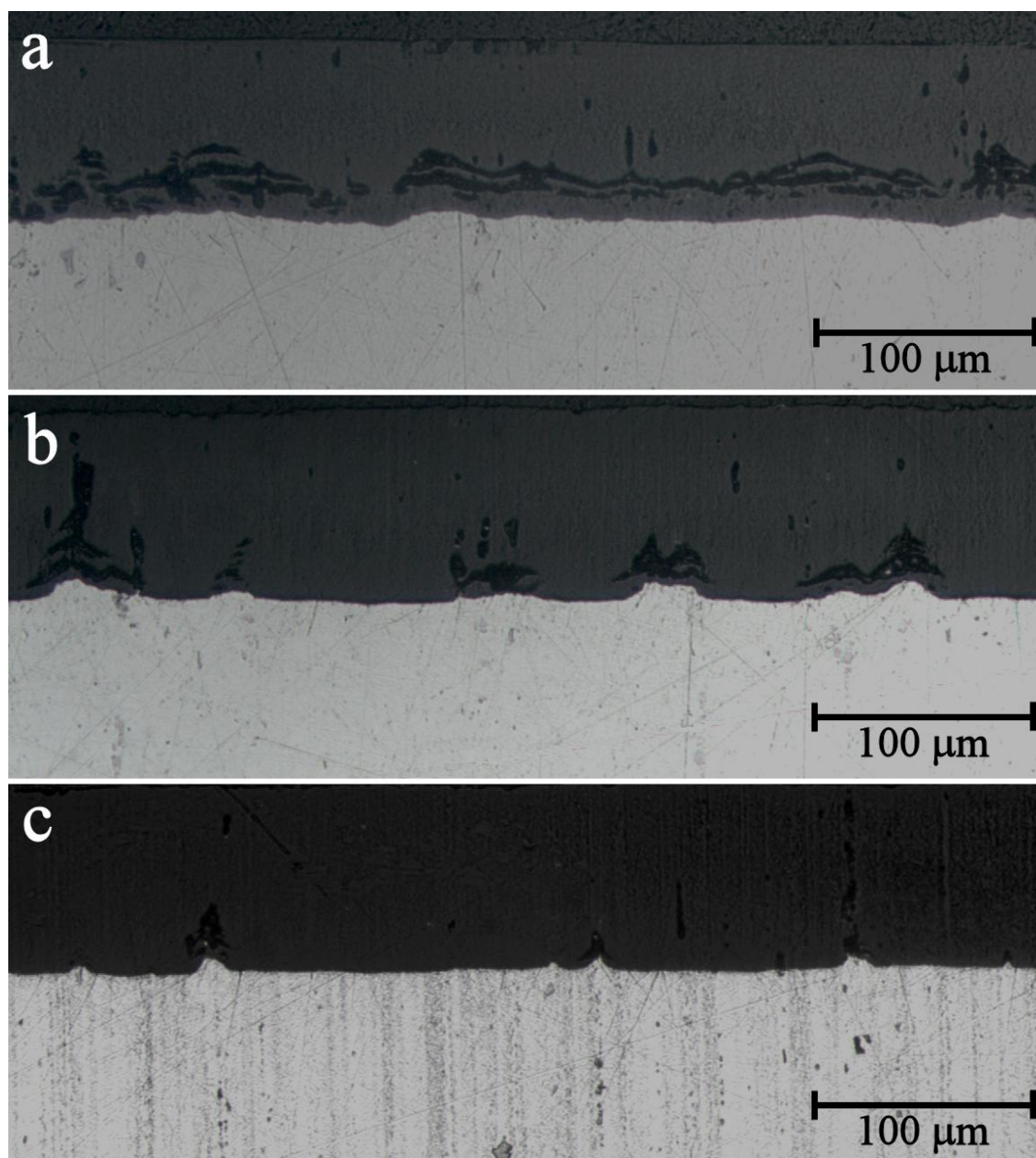
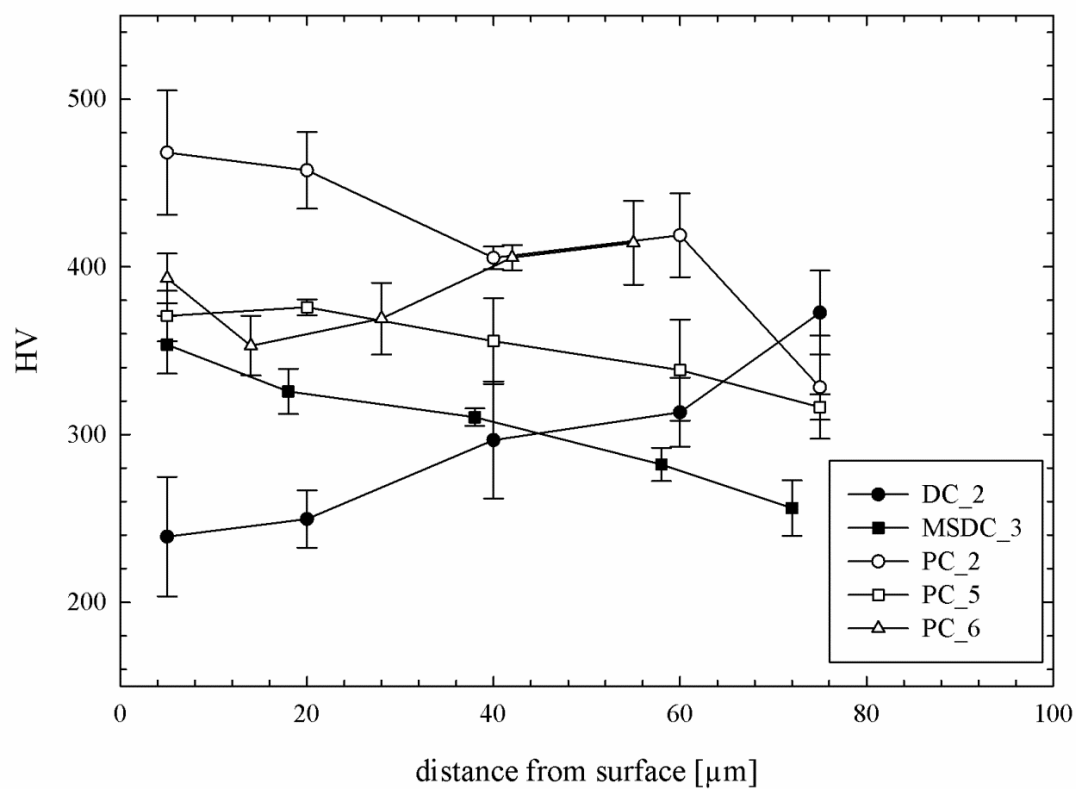
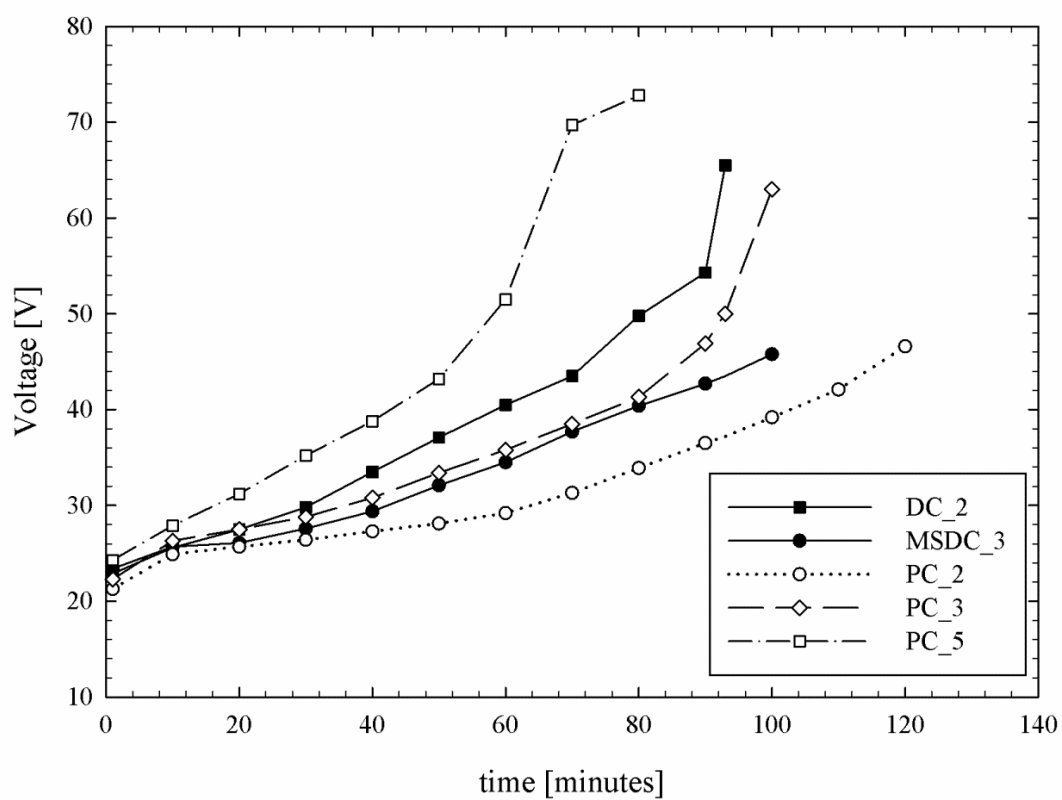


Figure 3

**Figure 4**

**Figure 5**

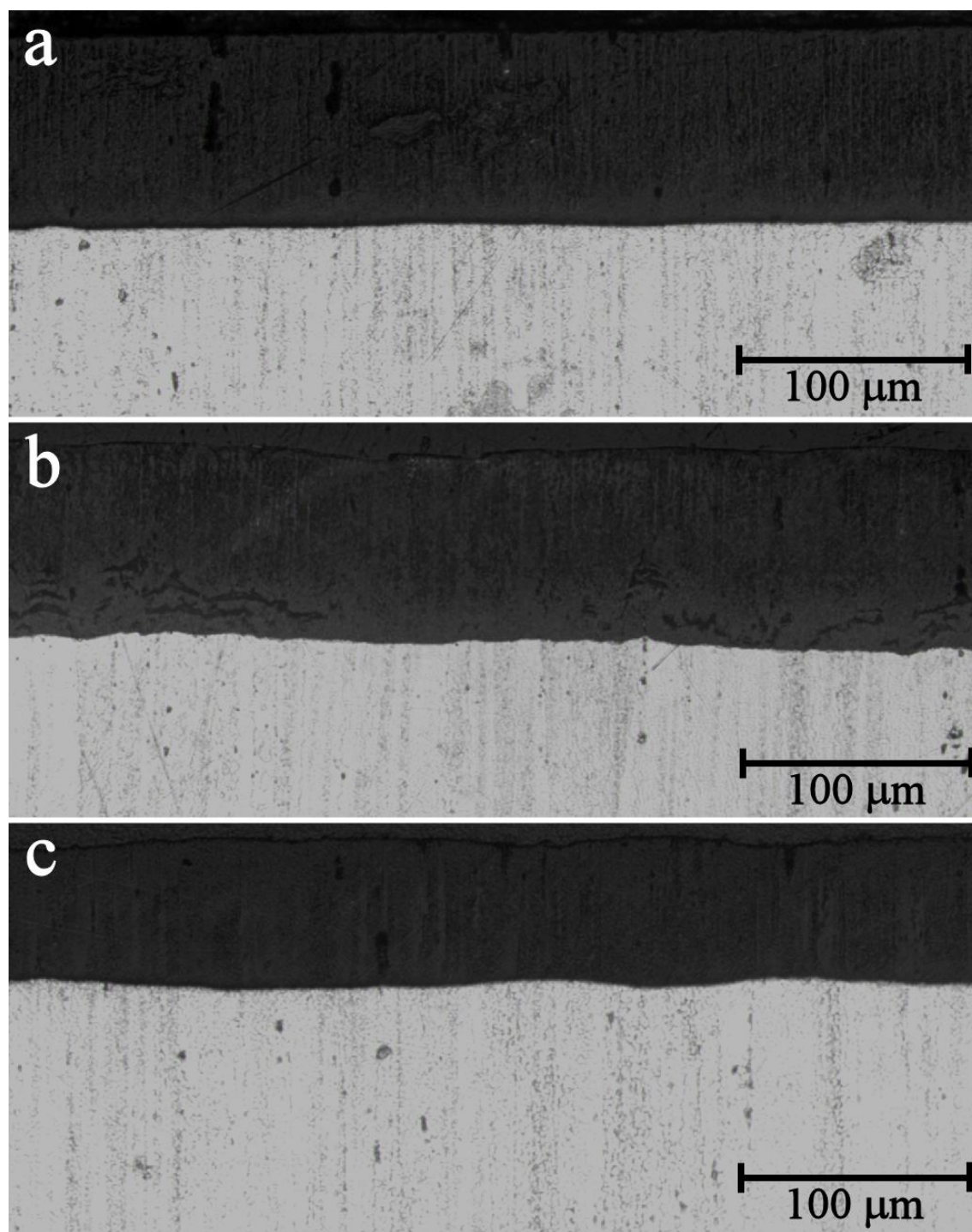


Figure 6

Highlights

- 1) electrical cycles to obtain hard and adherent anodic films on AA7075-T6 were defined
- 2) pulsed current procedures for homogenization of the oxide growth of AA7075-T6 were tested
- 3) temperature effect on direct current hard anodizing of AA7075-T6 was studied